



## RESEARCH ARTICLE OPEN ACCESS

# Precision RNAi in Tomato Using Synthetic Trans-Acting Small Interfering RNAs Derived From Minimal Precursors

Ariel H. Tomassi | María Juárez-Molina | Adriana E. Cisneros | Ana Alarcia | Francesca Orlando | Sara Toledano-Franco | Silvia Presa | Antonio Granell | Alberto Carbonell

Instituto de Biología Molecular y Celular de Plantas, Consejo Superior de Investigaciones Científicas–Universitat Politècnica de València, Valencia, Spain

**Correspondence:** Alberto Carbonell ([acarbonell@ibmcp.upv.es](mailto:acarbonell@ibmcp.upv.es))

**Received:** 10 April 2025 | **Revised:** 25 September 2025 | **Accepted:** 30 September 2025

**Funding:** This work was supported by HORIZON Europe Marie Skłodowska-Curie Actions (HORIZON-MSCA-2023-PF-01-101149036), MCIN, AEI and NextGenerationEU/PRTR (CNS2022-135107, PDC2022-133241-I00, PID2021-122186OB-I00 and PID2024-155602OB-I00).

**Keywords:** antiviral resistance | functional genomics | gene silencing | PVX | RNAi | syn-tasiRNA | tomato | TSWV

## ABSTRACT

RNA interference (RNAi) is a highly conserved gene silencing mechanism regulating gene expression at transcriptional and post-transcriptional levels in plants. Synthetic trans-acting small interfering RNAs (syn-tasiRNAs) have emerged as powerful tools for highly specific and efficient gene silencing. However, their application in crops has been constrained by the need for transgene integration and the relatively long length of *TAS*-derived precursors. Here, we developed a novel syn-tasiRNA platform for *Solanum lycopersicum* (tomato) based on minimal precursors targeted by endogenous SlmiR482b microRNA. These minimal precursors, comprising only a 22-nt miRNA target site, an 11-nt spacer, and the syn-tasiRNA sequence(s), effectively produced functional syn-tasiRNAs in both transgenic and transient virus-induced gene silencing (syn-tasiR-VIGS) systems. To facilitate their broader application, we engineered a series of vectors for high-throughput cloning and efficient syn-tasiRNA expression from SlmiR482b-based minimal precursors in tomato. Our results show that minimal precursors induce robust gene silencing of endogenous tomato genes and confer antiviral resistance to the economically important tomato spotted wilt virus. Furthermore, we show that syn-tasiR-VIGS can be applied in a transgene-free manner through crude extract delivery, leading to efficient silencing of endogenous genes. This study establishes minimal syn-tasiRNA precursors as a versatile and efficient tool for precision RNAi in tomato, with applications in functional genomics and crop improvement.

## 1 | Introduction

RNA interference (RNAi) is an evolutionarily conserved mechanism that regulates gene expression through the sequence-specific degradation or translational repression of target messenger RNAs (mRNAs) by complementary 20- to 24-nucleotide (nt) small RNA (sRNA) molecules (Fire et al. 1998; Hannon 2002). RNAi is initiated by the processing of double-stranded RNA (dsRNA) into small interfering RNAs (siRNAs)

or microRNAs (miRNAs) by Dicer ribonucleases (Bernstein et al. 2001; Hammond et al. 2000). These sRNAs are subsequently incorporated into an ARGONAUTE (AGO)-containing RNA-induced silencing complex (RISC), which recognises complementary mRNA sequences and directs their cleavage or translational suppression (Bartel 2004; Bernstein et al. 2001). In plants, RNAi plays fundamental roles in endogenous gene regulation, antiviral immunity, transposon silencing, and defence against pathogens (Baulcombe 2004; Ding and Voinnet 2007).

Ariel H. Tomassi and María Juárez-Molina contributed equally to this study.

This is an open access article under the terms of the [Creative Commons Attribution](https://creativecommons.org/licenses/by/4.0/) License, which permits use, distribution and reproduction in any medium, provided the original work is properly cited.

© 2025 The Author(s). *Plant Biotechnology Journal* published by Society for Experimental Biology and The Association of Applied Biologists and John Wiley & Sons Ltd.

Classic RNAi-based approaches in plants involve the expression of dsRNA or hairpin RNA (hpRNA) transgenes to generate siRNAs homologous to the target gene(s) or the use of virus-induced gene silencing (VIGS) vectors. While effective, these methods generate heterogeneous siRNA populations, increasing the likelihood of off-target effects (Jackson et al. 2003). More recently, second-generation RNAi strategies based on 21-nt artificial sRNAs (art-sRNAs) were developed to improve specificity. Art-sRNAs are computationally designed to selectively target and cleave RNA transcripts with high specificity while minimising off-target interactions (Carbonell 2017). Art-sRNAs are categorised into two major classes: artificial microRNAs (amiRNAs) and synthetic trans-acting small interfering RNAs (syn-tasiRNAs), which operate through similar mechanisms but differ in their biogenesis. AmiRNAs are generated from *MIR* transgenes in which endogenous miRNA and miRNA\* sequences are replaced with engineered amiRNA and amiRNA\* sequences. Conversely, syn-tasiRNAs are derived from *TAS* transgenes, allowing the simultaneous production of multiple syn-tasiRNAs from a single precursor, facilitating multi-site targeting within one or more transcripts. Briefly, the endogenous tasiRNA sequences of *TAS* transgenes are replaced with one or more 21-nt syn-tasiRNA sequences arranged in tandem, each designed to target specific genes of interest (Zhang 2014). *TAS* transgenes are transcribed in the nucleus by DNA-dependent RNA polymerase II, producing a primary *TAS* transcript (*TAS* precursor) that contains a 5' cap, a polyadenylated tail and a miRNA-specific target site (TS), typically 22-nt in length (Chen et al. 2010; Cuperus et al. 2010). Once exported to the cytoplasm, the *TAS* precursor is cleaved by a 22-nt miRNA/AGO complex, generating a fragment stabilised by SUPPRESSOR OF GENE SILENCING 3 (SGS3), preventing its degradation and allowing RNA-DEPENDENT RNA POLYMERASE 6 (RDR6) to synthesise a complementary dsRNA (Allen et al. 2005; Yoshikawa et al. 2005). This dsRNA is then processed into phased 21-nt syn-tasiRNA duplexes by DCL4, following a pathway similar to that of endogenous tasiRNAs. Finally, HUA ENHANCER1 (HEN1) methylates the 3' ends of both strands, stabilising them before the guide strand is incorporated into AGO1 (Li et al. 2005).

Despite their potential in functional genomics and crop improvement, syn-tasiRNA applications have been constrained by the need for *TAS*-based transgene integration, which is labour-intensive and raises regulatory concerns associated with genetically modified plants (Su et al. 2023). Furthermore, the relatively long length of *TAS*-derived precursors can increase RNA synthesis costs and reduce stability in viral vectors, as observed for full-length *MIR390a* and *TAS1c* amiRNA and syn-tasiRNA precursors, respectively, in *Arabidopsis thaliana* (Arabidopsis) and *Nicotiana benthamiana* (Cisneros, Martín-García, et al. 2023; Cisneros et al. 2025). These limitations have been recently overcome by the development of non-*TAS* syn-tasiRNA precursors of minimal length, termed “minimal” precursors, consisting of a 22-nt endogenous miRNA TS, an 11-nt spacer and the 21-nt syn-tasiRNA sequence(s). These minimal precursors were shown to generate functional syn-tasiRNAs and induce effective gene silencing when stably expressed in transgenic Arabidopsis or transiently expressed in *N. benthamiana* (Cisneros et al. 2025). Remarkably, they also produced authentic syn-tasiRNAs and induced widespread gene silencing in *N. benthamiana* when expressed from an RNA virus, a strategy named syn-tasiR-VIGS

(Cisneros et al. 2025). However, whether syn-tasiRNAs can be efficiently processed and applied for stable and transgene-free gene silencing in crop species remains an open question.

In this study, we developed a syn-tasiRNA system for *Solanum lycopersicum* (tomato) using minimal precursors incorporating a SlmiR482b TS followed by an 11-nt spacer and the 21-nt syn-tasiRNA sequence(s). We show that authentic and highly effective syn-tasiRNAs can be produced from these minimal, non-*TAS* precursors in both transgenic plants and syn-tasiR-VIGS systems. Furthermore, minimal precursors successfully silenced endogenous genes and induced antiviral resistance against tomato spotted wilt virus (TSWV). Finally, we show that transgene-free syn-tasiR-VIGS, when delivered as crude extracts, resulted in efficient silencing of tomato genes. Collectively, these results establish syn-tasiRNAs as a powerful and versatile tool for gene silencing in tomato.

## 2 | Results

### 2.1 | Syn-tasiRNA Production in *S. lycopersicum* From Minimal Precursors Using Endogenous 22-Nt miRNA Triggers

To develop a functional syn-tasiRNA platform in *S. lycopersicum*, we first identified endogenous 22-nt miRNAs capable of triggering secondary siRNA production. We focused on SlmiR482b and SlmiR6020, both of which target nucleotide binding leucine-rich repeat (NLR) immune receptor genes and initiate phased secondary siRNA biogenesis from target transcripts (Deng, Muhammad, et al. 2018; Shivaprasad et al. 2012). Next, to assess syn-tasiRNA production in tomato, the *35S:SlmiR482bTS-NbSu* and *35S:SlmiR6020TS-NbSu* constructs were generated for expressing syn-tasiR-NbSu – a syn-tasiRNA targeting the *Nicotiana benthamiana* *SULPHUR* (*NbSu*) gene that accumulates to high levels in plant tissues (Cisneros et al. 2022) from minimal precursors including SlmiR482b or SlmiR6020 TS, respectively (Figure 1A). Agroinfiltration of these constructs was performed in separate areas of two leaves from three different tomato plants. Negative control constructs *35S:SlmiR482b-GUS<sub>Nb</sub>* and *35S:SlmiR6020-GUS<sub>Nb</sub>* were designed to produce syn-tasiR-GUS<sub>Nb</sub>, a syn-tasiRNA targeting *Escherichia coli uidA* β-glucuronidase gene (or *GUS*), from minimal precursors targeted by SlmiR482b and SlmiR6020, respectively (Figure 1A). As a positive control, the *35S:AtTAS1c-NbSu/AtMIR173A* construct was used, as it is known to efficiently produce *AtTAS1c*-based syn-tasiRNAs in tomato due to the co-expression of *Arabidopsis thaliana* AtmiR173a 22-nt miRNA (López-Dolz et al. 2020).

RNA blot analysis of agroinfiltrated leaf samples collected at 2 days post-agroinfiltration (dpa) revealed high syn-tasiR-NbSu accumulation in samples expressing the *SlmiR482bTS*-based precursor, comparable to levels observed in positive control samples co-expressing *AtTAS1c-NbSu* and *AtMIR173a* (Figure 1B). In contrast, syn-tasiR-NbSu accumulated to barely detectable levels in samples expressing *SlmiR6020TS*-based minimal precursors, and, as expected, no syn-tasiR-NbSu was detected in negative control samples (Figure 1B). High-throughput sequencing of sRNAs from *35S:SlmiR482bTS-NbSu* and *35S:AtTAS1c-NbSu/AtMIR173a* samples confirmed that both precursors were

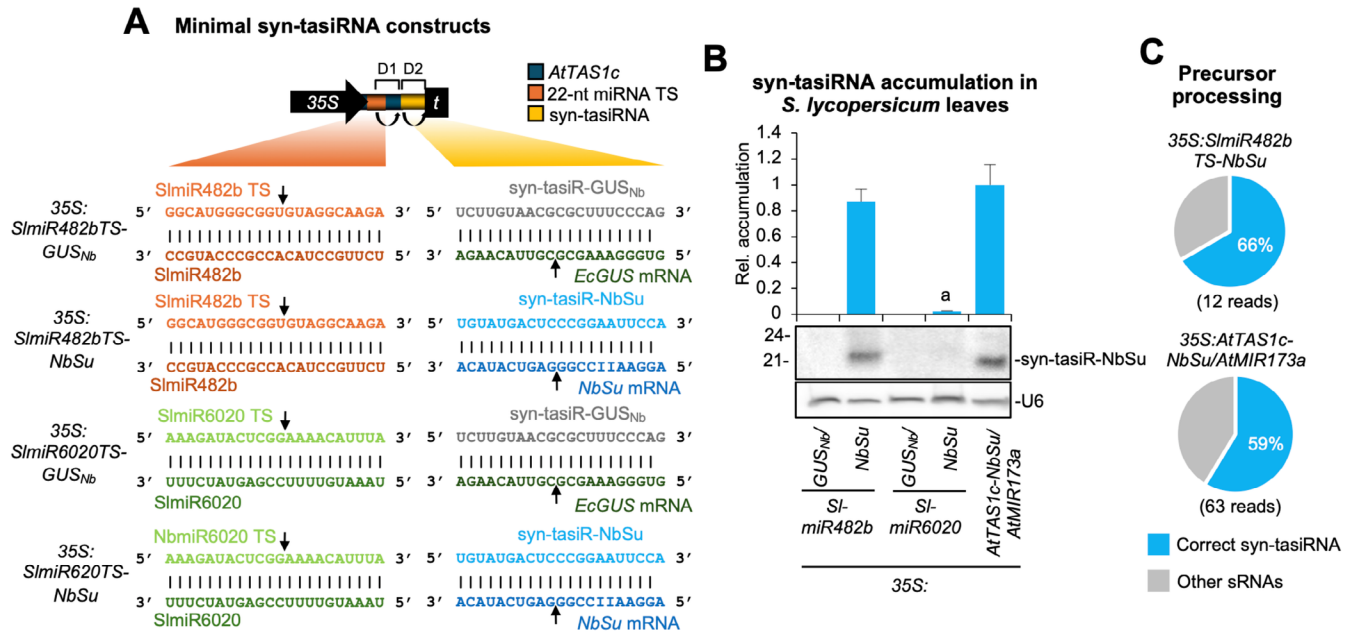


**FIGURE 1** | Accumulation in *Solanum lycopersicum* leaves of syn-tasiRNAs expressed from minimal precursors including endogenous 22-nt miRNA target sites (TS). (A) Organisation of minimal precursor constructs. Nucleotides (nt) corresponding to SlmiR482b and SlmiR6020 TSs are shown in light orange and green, respectively. Nucleotides corresponding to SlmiR482b and SlmiR6020 are shown in dark orange and green, respectively. Nucleotides corresponding to syn-tasiR-GUS<sub>Nb</sub> and syn-tasiR-NbSu are shown in light grey and blue, while those of their target mRNAs are shown in dark grey and blue, respectively. Arrows indicate the predicted cleavage sites for endogenous 22-nt miRNAs and syn-tasiRNAs. (B) Northern blot detection of syn-tasiR-NbSu in RNA preparations from agroinfiltrated leaves collected 2 days post-agroinfiltration. The graph at top shows the mean + standard deviation ( $n = 3$ ) syn-tasiRNA relative accumulation (35S:AtTAS1c-NbSu/MIR173 = 1). Bar with the letter “a” is significantly different from that of 35S:AtTAS1c-NbSu/MIR173 control samples. Each biological replicate is a pool of six agroinfiltrated leaves. One blot from three biological replicates is shown. U6 blot is shown as loading control. (C) Syn-tasiRNA processing from minimal precursors and controls. Pie charts show the percentages of reads corresponding to expected, accurately processed 21-nt mature syn-tasiR-NbSu (in blue) or to other 19–24 nts sRNAs (in grey).

processed with similar accuracy. The majority of reads within  $\pm 4$  nt of the 3’D2[+] position (66% and 59%, respectively) corresponded to authentic syn-tasiR-NbSu (Figure 1C). These results demonstrate that SlmiR482b can efficiently trigger syn-tasiRNA production in tomato from minimal precursors, providing a basis for the development of an optimised syn-tasiRNA system for this species.

## 2.2 | High-Throughput B/c Vectors for Syn-tasiRNA Expression in Tomato

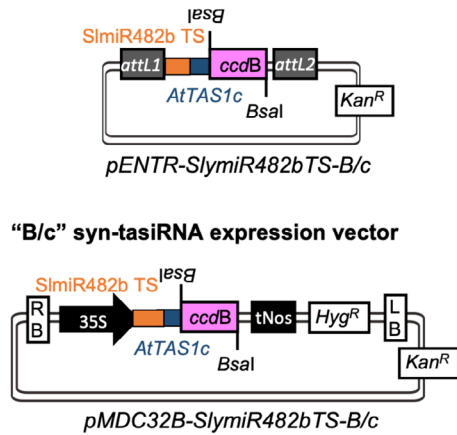
To facilitate high-throughput cloning and expression of syn-tasiRNAs in tomato, we developed two new “B/c” vectors incorporating SlmiR482b: (i) *pENTR-SlmiR482bTS-B/c*, a Gateway-compatible entry vector allowing the direct insertion of syn-tasiRNA sequences and subsequent recombination into preferred expression vectors with customisable promoters, terminators and regulatory elements and (ii) *pMDC32B-SlmiR482bTS-B/c*, a binary vector for direct transformation, eliminating the need for intermediate subcloning steps (Figure 2A). Both vectors contain the SlmiR482b TS followed by an 11-nt spacer sequence derived from *AtTAS1c* and a 1461 bp DNA cassette encoding the control of cell death (*ccdB*) gene (Bernard and Couturier 1992), flanked by two inverted *BsaI* restriction sites downstream of the 3’D1[+] position (Figure 2A). Syn-tasiRNA constructs were generated

using a simplified and cost-effective cloning method, following established protocols for B/c-based vectors (Carbonell et al. 2014; Cisneros et al. 2025). Briefly, syn-tasiRNA inserts were generated by annealing two 25-nt overlapping and partially complementary oligonucleotides containing the syn-tasiRNA sequence, with 5’-TTTA and 5’-CCGA overhangs. These were then directionally ligated into *BsaI*-digested *SlmiR482bTS-B/c* vectors (Figure S1 and Protocol S1). The configuration of *SlmiR482bTS*-based syn-tasiRNA constructs expressing a single syn-tasiRNA is illustrated in Figure 2B. These vectors were subsequently used throughout the study to evaluate gene silencing efficacy of syn-tasiRNAs expressed from *SlmiR482bTS*-based minimal precursors.

## 2.3 | Generation of Delayed Flowering Transgenic Tomato Plants Expressing a Syn-tasiRNA Against *SISFT*

To determine whether syn-tasiRNAs expressed from *SlmiR482bTS*-based precursors could efficiently downregulate endogenous genes in tomato, we targeted the *SINGLE FLOWER TRUSS (SISFT)* gene, a key regulator of flowering time (Krieger et al. 2010). The 21-nt syn-tasiR-SISFT sequence, previously shown to silence *SISFT* when expressed as an artificial miRNA (Jiang et al. 2013; Shalit et al. 2009), was cloned into the *pMDC32B-SlmiR482bTS-B/c* vector. The resulting construct,

## A Gateway-compatible “B/c” entry vectors



## B *SlmiR482b*-based syn-tasiRNA constructs

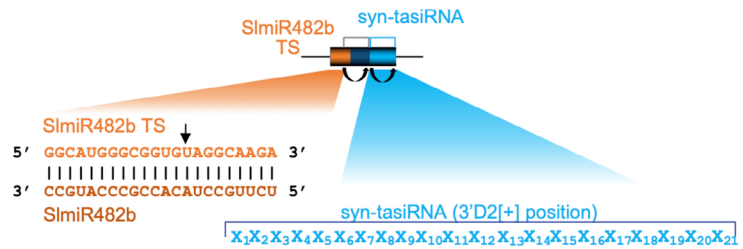


**FIGURE 2** | B/c-based vectors for direct cloning of syn-tasiRNAs downstream *SlmiR482b* target site (TS). (A) TS is in orange, the spacer sequence derived from *AtTAS1c* is in blue. Top, diagram of the Gateway-compatible entry vectors. Bottom, diagram of binary vector for in plant expression of syn-tasiRNAs. RB: Right border; 35S: Cauliflower mosaic virus promoter; *BsaI*: *BsaI* recognition site, *ccdB*: Gene encoding the gyrase toxin, in pink; LB: Left border; attL1 and attL2: GATEWAY recombination sites. *Kan<sup>R</sup>*: Kanamycin resistance gene; *Hyg<sup>R</sup>*: Hygromycin resistance gene. (B) Organisation of *SlmiR482b*-based syn-tasiRNA constructs. Base pairing between *SlmiR482b* (dark orange) and its target site (light orange) nucleotides is shown. Curved black arrows indicate DCL4 processing sites. Black linear arrows indicate sRNA-guided cleavage sites. TS refers to target site. In the example diagram, one single 21-nt guide syn-tasiRNA sequence was introduced at the 3'D2[+] position in *SlmiR482bTS*-based precursors.

35S:*SlmiR482bTS-SISFT* (Figure 3A), was introduced into tomato cotyledon explants via *Agrobacterium*-mediated transformation. Importantly, successful expression of syn-tasiR-SISFT in transgenic plants was expected to effectively downregulate *SISFT*, resulting in a delayed flowering phenotype. This trait holds significant agronomic potential, as it could extend the fruit-setting period, synchronise production with market demand, and provide an extended window for crossing in breeding programmes.

Phenotypic analysis of six independent T1 transgenic lines at 5 weeks post-transplanting (wpt) revealed a significant delay in flowering compared to non-transgenic control (NTC) plants (Figure 3B). While NTC plants produced an average of 10 leaves before the emergence of the first inflorescence (I1), syn-tasiR-SISFT-expressing transgenic lines exhibited an increased number of leaves (13–15) before I1 formation (Figure 3C), confirming a delayed transition from the vegetative to the reproductive phase. To assess the molecular effects of syn-tasiR-SISFT, RT-qPCR analysis was performed at 12 wpt to measure *SISFT* transcript levels. Our results show a significant reduction in *SISFT* mRNA accumulation in syn-tasiR-SISFT-expressing plants compared to NTCs (Figure 3D), indicating effective suppression of *SISFT* expression. To confirm that the reduced *SISFT* transcript levels were due to syn-tasiR-SISFT-mediated cleavage, 5'-RLM-RACE analysis was conducted. Gel electrophoresis confirmed the amplification of the expected 3' cleavage fragments in transgenic plants, whereas no cleavage products were detected in NTC samples (Figure 3E, lower panel). Sequence analysis of 5'-RLM-RACE products revealed precise cleavage at the expected target site within the *SISFT* mRNA, with a high proportion of cleavage events occurring at the predicted position (Figure 3E, upper panel). RT-PCR analysis further confirmed the downregulation of *SISFT* in transgenic plants, while *SIAC* expression

was used as a reference to validate RNA integrity and cDNA synthesis across all samples. Collectively, these results demonstrate that syn-tasiR-SISFT, produced from *SlmiR482bTS*-based minimal precursors, effectively downregulates *SISFT* in transgenic tomato plants, leading to a prolonged vegetative phase and a delayed flowering.

Next, to assess the accumulation and processing efficiency of syn-tasiR-SISFT, northern blot analysis of RNA preparations from apical leaves at 12 wpt confirmed the presence of a 21-nt RNA species corresponding to syn-tasiR-SISFT in transgenic lines, whereas no detectable signal was observed in NTC plants (Figure 4A). High-throughput sRNA sequencing further confirmed that syn-tasiR-SISFT was accurately processed. Analysis of 19- to 24-nt reads mapping to *SlmiR482bTS-SISFT* precursors revealed a major peak corresponding to 21-nt reads starting at the expected syn-tasiRNA position (position 34) and corresponding to syn-tasiR-SISFT (Figure 4B). Additionally, 87% of reads within  $\pm 4$  nt of the 3'D2[+] position corresponded to authentic syn-tasiR-SISFT, with only a minor fraction mapping to other regions (Figure 4C), indicating that *SlmiR482bTS*-based precursors are efficiently recognised and cleaved in tomato. To further evaluate the phased processing of the syn-tasiRNA precursor, we analysed the register distribution of 21-nt reads along the precursor transcript. A radar plot showed that 98% of 21-nt reads aligned to the expected register, confirming that tasiRNA processing occurs with high phasing precision in tomato (Figure 4D). Finally, the absence of 21-nt siRNAs derived from *SISFT* (Figure S2, Data S1) indicates that syn-tasiR-SISFT is only causing the intended cleavage of *SISFT*, without triggering an amplification loop of secondary, 21-nt siRNAs that could target other regions of the mRNA or similar sequences. Together, these results confirm that syn-tasiR-SISFT is stably expressed, accurately processed from *SlmiR482bTS*-based minimal precursors, and induces specific and robust gene silencing in tomato.

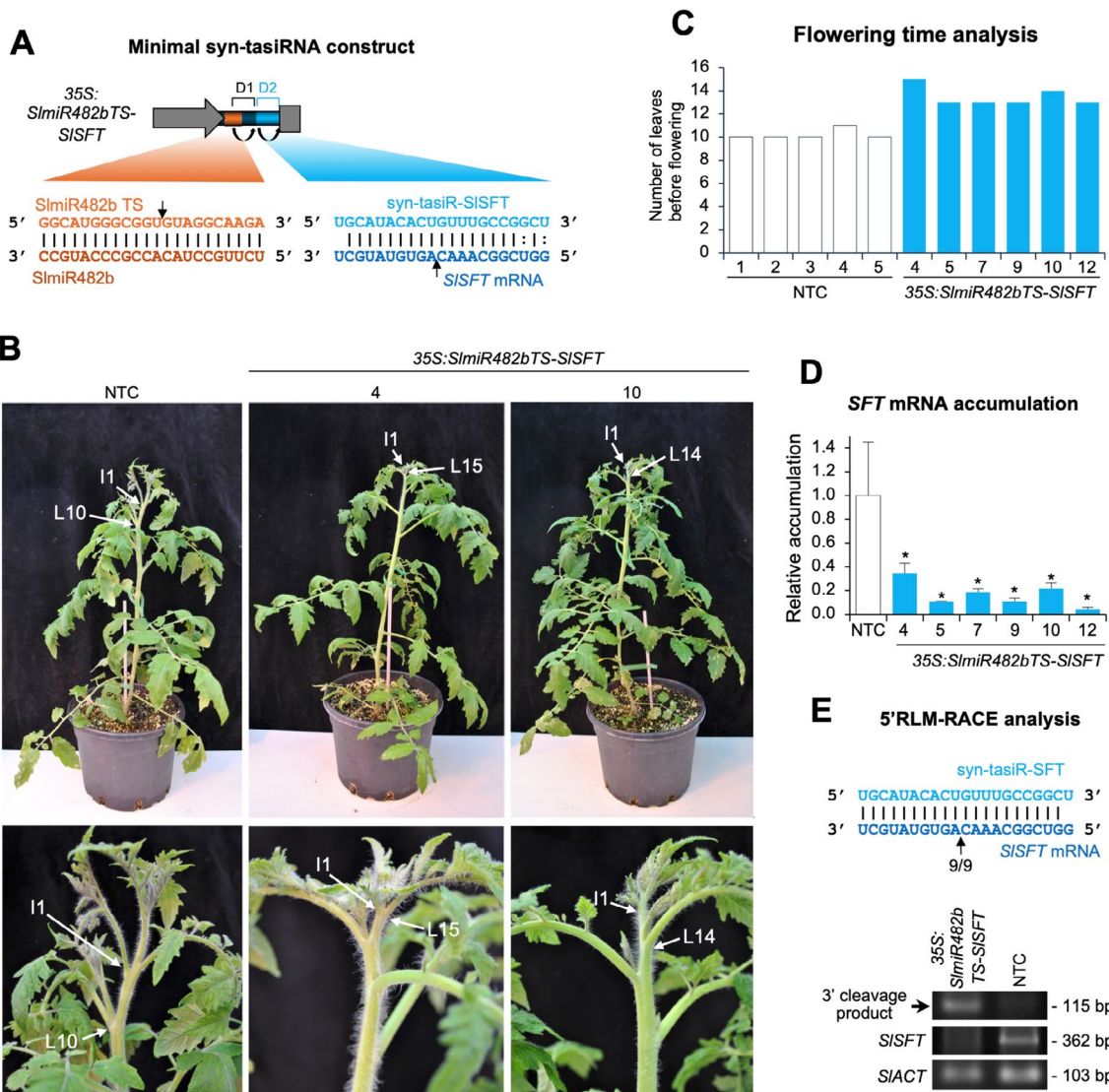


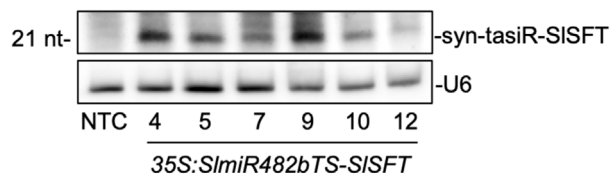
**FIGURE 3** | Functional analysis of *Solanum lycopersicum* T1 transgenic lines expressing syn-tasiR-SISFT, a syn-tasiRNA targeting *SINGLE FLOWER TRUSS* (*SISFT*). (A) Schematic representation of the anti-*SISFT* syn-tasiRNA construct, 35S:*SlmiR482bTS-Sisft*, engineered to express syn-tasiR-SISFT (light blue) from a minimal precursor containing the *SlmiR482b* target site (TS) (orange) and a 11-nt spacer derived from *AtTAS1c* (dark blue). Other details are as described in Figure 1A. (B) Photographs taken at 5 weeks post-transplanting (wpt) of representative transgenic tomato lines expressing anti-*SISFT* syn-tasiRNA compared to a non-transgenic control (NTC) plant. Top panel: Whole plants. Bottom panel: Detail of the apical region, with arrows marking the first emerging inflorescence (I1) and the last leaf (L), numbered, before it. (C) Phenotypic analysis of flowering time in NTC and syn-tasiRNA transgenic lines, showing the number of leaves present at the time of the first emerging inflorescence in each plant. (D) Accumulation of *SISFT* mRNA in tomato plants. Data are presented as the mean + SE relative expression levels of *SISFT* mRNA at 12 wpt after normalisation to *Actin* (*SIACT*), as determined by RT-qPCR (NTC = 1 in all comparisons). The asterisk indicates a significant difference from the NTC samples ( $p < 0.05$ ; pairwise Student's *t*-test comparison). The NTC sample corresponds to a pooled sample from five NTCs. (E) 5'-RLM-RACE analysis of syn-tasiR-SISFT-guided cleavage of *SISFT*. Upper panel: Predicted base pairing between syn-tasiR-SISFT and *SISFT* mRNA, with the expected cleavage site indicated by an arrow. The proportion of cloned 5'-RLM-RACE products at the expected cleavage site is shown for syn-tasiR-SISFT-expressing lines. Lower panel: Ethidium bromide-stained gel showing 5'-RLM-RACE products corresponding to the 3' cleavage product from syn-tasiR-SISFT-guided cleavage (top), along with RT-PCR products for the target *SISFT* (middle) and the control *SIACT* genes (bottom). The position and expected sizes of syn-tasiRNA-based 5'-RLM-RACE products and control RT-PCR products are indicated.

## 2.4 | Syn-tasiR-VIGS Antiviral Vaccination of Tomato Plants Against TSWV

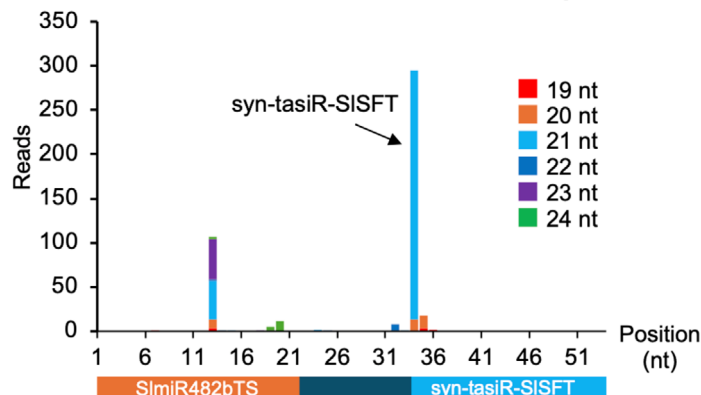
Next, to evaluate the potential of using a viral vector for syn-tasiRNA-mediated gene silencing in tomato, we investigated the efficacy of potato virus X (PVX)-based syn-tasiR-VIGS to confer resistance against tomato spotted wilt virus (TSWV).

Several PVX-based constructs were generated for expressing syn-tasiRNAs from minimal precursors (Figure 5A). The 35S:PVX-*SlmiR482bTS-TSWV(x4)* construct included the *SlmiR482bTS* precursor engineered to produce four highly active syn-tasiRNAs (syn-tasiR-TSWV-1 to syn-tasiR-TSWV-4) targeting conserved regions of the TSWV genome (Carbonell, Lisón, and Daròs 2019; Carbonell, Lopez, and Daròs 2019)

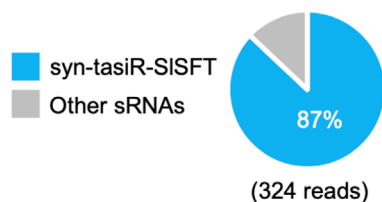
## A syn-tasiR-SISFT accumulation in transgenic tomato leaves



## B sRNAs derived from *SlmiR482bTS-SISFT* precursor



## C Precursor processing



## D Phasing analysis

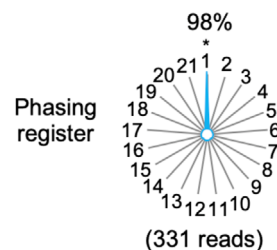


**FIGURE 4** | Accumulation and processing of syn-tasiR-SISFT expressed from *SlmiR482bTS*-based precursors in *Solanum lycopersicum* T1 transgenic lines. (A) Northern blot detection of syn-tasiR-SISFT in RNA preparations from apical leaves collected 12 weeks post-transplanting from six independent transgenic lines and one non-transgenic control (NTC). Each sample represents a pool of two apical leaves. Other details are as described in Figure 1B. (B) sRNA profile of 19–24 nt [+] reads mapping to each of the 54 nucleotide positions within the *SlmiR482bTS-SISFT* precursor from plants expressing *35S:SlmiR482bTS-SISFT*. Orange, dark blue and light blue boxes represent nucleotides corresponding to *NbmiR482aTS*, the *AtTAS1c*-derived spacer and syn-tasiR-SISFT, respectively. (C) Pie chart showing the percentage of reads corresponding to accurately processed 21-nt authentic syn-tasiR-SISFT (blue) versus other 19–24-nt sRNAs (grey). (D) Radar plot displaying the distribution of 21-nt reads across the 21 registers of the precursor transcripts, with position 1 designated immediately after the *SlmiR482b*-guided cleavage site.

(Figure 5B). Negative control constructs included the *35S:PVX-SlmiR482bTS-GUS<sub>Sl</sub>(x4)* construct, designed to express two syn-tasiRNAs (syn-tasiR-GUS<sub>Sl</sub>-1 and syn-tasiR-GUS<sub>Sl</sub>-2) against *GUS* (with no off-targets in tomato) (Carbonell, Lisón, and Daròs 2019) from *SlmiR482bTS*-based precursors, and *35S:PVX-AtmiR173aTS-TSWV(x4)*, including the *AtmiR173a* TS, which was expected to fail in triggering syn-tasiRNA biogenesis due to the absence of *AtmiR173a* in *S. lycopersicum* (Figure 5B), as reported before in *N. benthamiana* (Cisneros et al. 2025).

To assess the antiviral activity of PVX-based constructs, each construct was agroinoculated into two leaves of six independent plants. Twelve days later, these same plants were further inoculated with TSWV, and symptom progression was

monitored over 28 days. At 14 days post inoculation (dpi), all plants expressing *35S:PVX-SlmiR482bTS-TSWV(x4)* remained asymptomatic, whereas control plants agroinoculated with *35S:PVX-SlmiR482bTS-GUS<sub>Sl</sub>(x4)* or *35S:PVX-AtmiR173aTS-TSWV(x4)* exhibited typical TSWV symptoms (Figure 5C,D), which developed and progressed similarly over time. Since plants from the two control blocks exhibited similar behaviour, subsequent molecular analyses were conducted comparing plants agroinoculated with *35S:PVX-SlmiR482bTS-TSWV(x4)* to those agroinoculated with *35S:PVX-SlmiR482bTS-GUS<sub>Sl</sub>(x4)*. At 14 dpi, western blot analysis revealed that four out of six plants expressing *35S:SlmiR482bTS-TSWV(x4)* did not accumulate detectable TSWV, while plants expressing *35S:SlmiR482bTS-GUS<sub>Sl</sub>(x4)* accumulated high TSWV levels (Figure 5E). By 28 dpi, two plants

expressing anti-TSWV syn-tasiRNAs from *SlmiR482bTS*-based precursors remained completely symptom-free (Figure 5C). Importantly, RT-PCR analysis confirmed the presence of a 341-bp fragment corresponding to the *SlmiR482bTS*-based precursors and a 230-bp fragment from the PVX coat protein (CP) in all PVX-treated samples, but not in mock-inoculated and non-agroinfiltrated plants, while a 235-bp fragment from *SITIP41*

was amplified in all samples (Figure 5F). Importantly, these results confirm that the lack of resistance in TSWV-infected plants was not caused by an absence of PVX infection or of the syn-tasiRNA precursor. Finally, northern blot analysis at 14 dpi confirmed the presence of high levels of 21-nt anti-TSWV syn-tasiRNAs in transgenic plants expressing *35S:SlmiR482bTS-TSWV(x4)*, whereas no corresponding signals were detected in

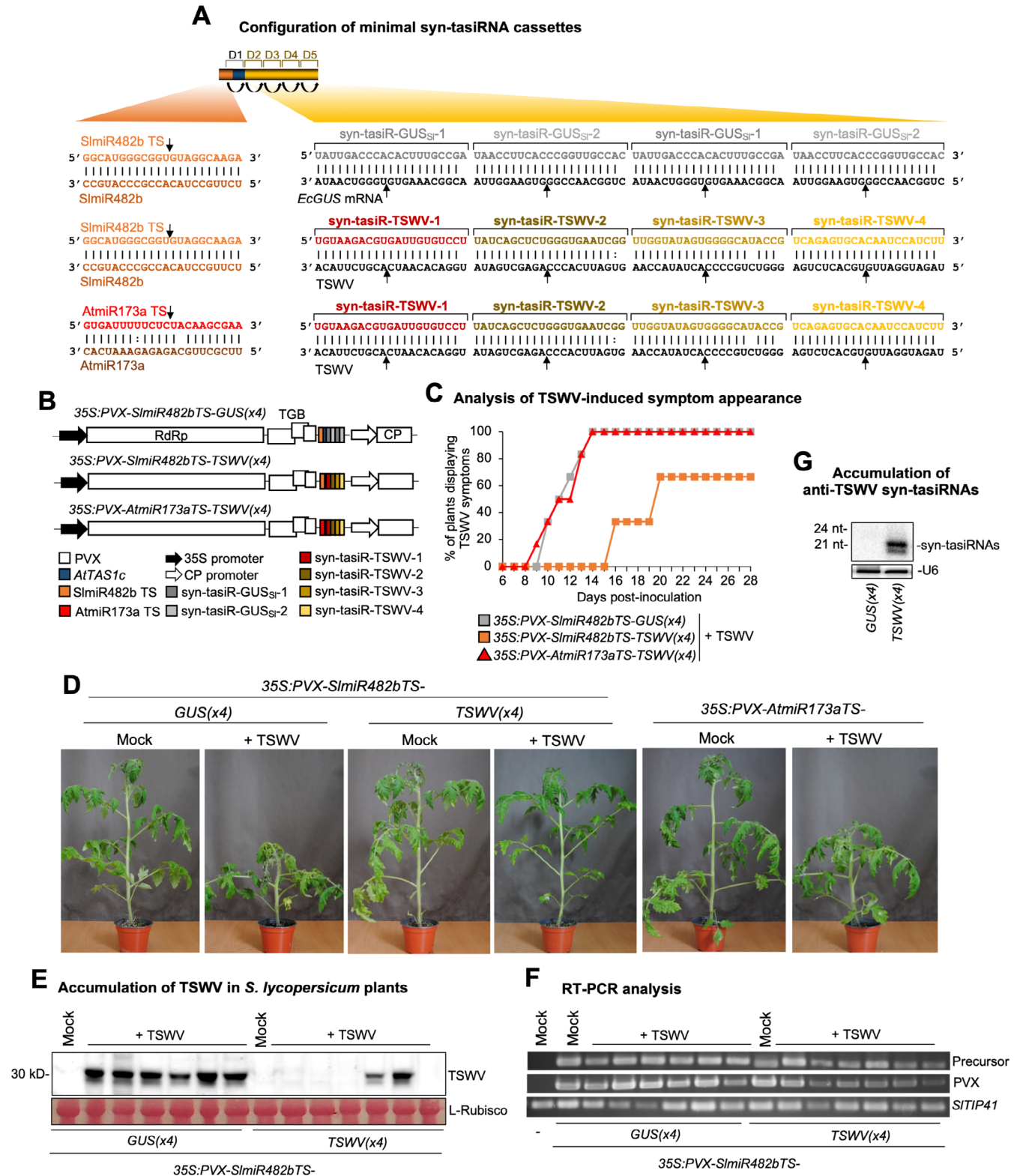


**FIGURE 5** | Legend on next page.

**FIGURE 5** | Functional analysis of potato virus X (PVX) constructs expressing syn-tasiRNAs against tomato spotted wilt virus (TSWV) in *S. lycopersicum*. (A) Schematic representation of PVX-based constructs. Nucleotides of anti-TSWV art-sRNA sequences syn-tasiR-TSWV-1, syn-tasiR-TSWV-2, syn-tasiR-TSWV-3 and syn-tasiR-TSWV-4 are in red, dark brown, light brown and yellow, respectively. Nucleotides of control anti-GUS art-sRNA sequences syn-tasiR-GUS<sub>Sl</sub>-1 and syn-tasiR-GUS<sub>Sl</sub>-2 are in dark and light grey, respectively. Nucleotides of AtmiR173a target site (TS) are in red and brown, respectively. Other details are as in Figure 1A. (B) Diagram of PVX-based constructs expressing anti-TSWV or anti-GUS syn-tasiRNAs. Colour coding for the syn-tasiRNA sequences is consistent with panel (A). Other details are as in Figure 1A. (C) Two-dimensional line graph showing, for each of the six-plant sets listed, the percentage of symptomatic plants per day during 28 days. (D) Photographs taken at 14 days post-inoculation (dpi) of plants agroinoculated with the different constructs and inoculated (+TSWV) or not (mock) with TSWV. (E) Western blot detection of TSWV in protein extracts from apical leaves collected at 14 dpi. A Ponceau-stained membrane is shown as a loading control, highlighting the large subunit of Rubisco (ribulose1,5-biphosphate carboxylase/oxygenase). (F) RT-PCR detection at 14 dpi of *SlmiR482bTS*-based precursors and PVX coat protein fragment (PVX-CP) in apical leaves agroinoculated plants. RT-PCR amplification of *SITYP41* is included as a control. (G) Northern blot detection of anti-TSWV art-sRNAs in RNA preparations from apical leaves collected at 14 dpi. A cocktail of probes to simultaneously detect syn-tasiR-TSWV-1, syn-tasiR-TSWV-2, syn-tasiR-TSWV-3 and syn-tasiR-TSWV-4 was used. Other details are as in Figure 1C.

35S:PVX-*SlmiR482bTS*-*GUS*<sub>Sl</sub>(x4) control samples (Figure 5G). These results indicate that syn-tasiRNA precursors were accurately processed and accumulated to levels sufficient for antiviral activity. Collectively, these results indicate that tomato vaccination with syn-tasiR-VIGS interferes with TSWV infection and can confer durable antiviral resistance.

## 2.5 | Transgene-Free Syn-tasiR-VIGS in Tomato

Next, we investigated the possibility of applying PVX-based syn-tasiR-VIGS in tomato in a transgene-free manner. Using P-SAMS (Fahlgren et al. 2016), we designed two highly specific syn-tasiRNAs (with no off-targets in *S. lycopersicum*) targeting *SULPHUR* (*SlSu*), a key enzyme in chlorophyll biosynthesis, or *1-DEOXY-D-XYLULOSE-5-PHOSPHATE SYNTHASE* (*SIDXS*), which plays a role in plastidic isoprenoid biosynthesis (Figure 6A). Silencing either gene was expected to induce bleaching phenotypes in tomato leaves. *SlmiR482bTS*-based precursors including these syn-tasiRNAs were inserted into a PVX infectious clone to generate the 35S:PVX-*SlmiR482bTS*-*SlSu*(x2) and 35S:PVX-*SlmiR482bTS*-*SIDXS*(x2) constructs (Figure 6B). The negative control 35S:PVX-*SlmiR482bTS*-*GUS*<sub>Sl</sub>(x2) construct including syn-tasiR-GUS<sub>Sl</sub>-1 and syn-tasiR-GUS<sub>Sl</sub>-2 sequences in tandem was also generated (Figure 6A,B). To prepare crude extracts for transgene-free syn-tasiR-VIGS, *Nicotiana benthamiana* plants were agroinfiltrated with PVX-based syn-tasiRNA constructs, and apical leaves were harvested 7 dpa for crude extract preparation (Figure 6C). These extracts were subsequently sprayed onto young tomato plants to induce silencing of *SlSu* or *SIDXS* (Figure 6C).

At 12 days post-spraying (dps), tomato plants treated with crude extracts containing anti-*SlSu* or anti-*SIDXS* syn-tasiRNAs developed small bleached spots on intermediate leaves, which expanded to cover most of the leaf surface at 14 dps and persisted until the end of the experiment at 28 dps, consistent with effective gene silencing (Figure 6D). Control plants sprayed with crude extracts containing control anti-*GUS* syn-tasiRNAs showed no bleaching, further confirming the specificity of syn-tasiRNA-mediated silencing. RT-qPCR analyses on RNA preparations from upper leaves at 14 dps revealed significantly reduced *SlSu* and *SIDXS* transcript levels in plants treated with PVX-*SlmiR482bTS*-*SlSu*(x2) or PVX-*SlmiR482bTS*-*SIDXS*(x2), respectively (Figure 6E), compared to controls. At this same

time point, RT-PCR analysis confirmed the presence of a 299-bp fragment corresponding to the *SlmiR482bTS*-based precursors and a 230-bp fragment from the PVX CP in all PVX-treated samples, but not in mock-inoculated plants, while a 103-bp fragment from *SLACT* was amplified in all samples (Figure 6F). Finally, northern blot analysis confirmed high accumulation of syn-tasiRNAs in these plants (Figure 6G). Taken together, these results show that syn-tasiRNAs can be efficiently produced from PVX crude extracts, accumulate to effective levels, and lead to robust and specific gene silencing in tomato in a transgene-free manner.

## 2.6 | Comparative Analysis of Minimal Syn-tasiRNA Precursor-Based Approaches With Other RNAi Strategies

We next compared the silencing efficiency of minimal syn-tasiRNA precursor-based approaches with other established RNAi strategies, including miRNA-induced gene silencing (MIGS) and the exogenous application of dsRNAs.

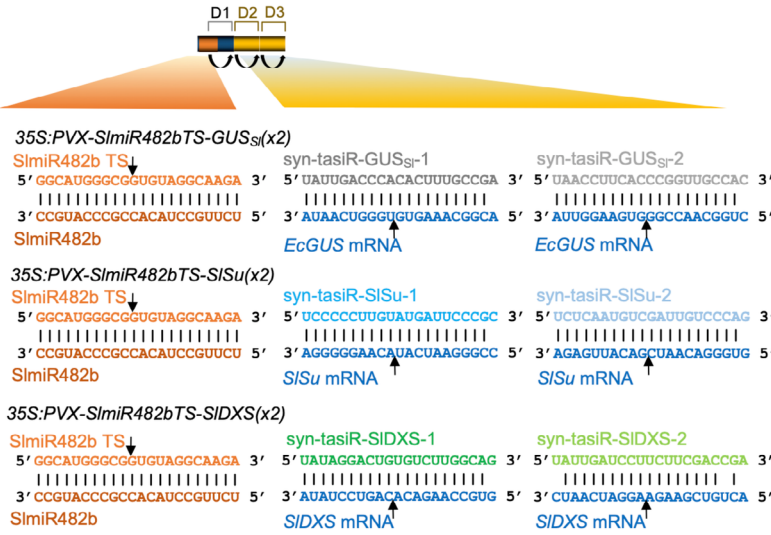
For MIGS, the 35S:*SlmiR482bTS*-*GUS*(MIGS), 35S:*SlmiR482bTS*-*SlSu*(MIGS), and 35S:*SlmiR482bTS*-*SIDXS*(MIGS) constructs were designed to express 402-, 414-, and 413-nt fragments of *GUS*, *SlSu* and *SIDXS*, respectively, downstream of the *SlmiR482bTS* TS (Figure S3A). These constructs were agroinfiltrated into separate areas of two leaves on each of three tomato plants. For comparison, the 35S:*SlmiR482bTS*-*GUS*<sub>Sl</sub>(x2), 35S:*SlmiR482bTS*-*SlSu*(x2) and 35S:*SlmiR482bTS*-*SIDXS*(x2) syn-tasiRNA constructs infiltrated in parallel. RT-qPCR analysis of target mRNA levels revealed a significant decrease in *SlSu* expression with both MIGS and syn-tasiRNA constructs, whereas *SIDXS* mRNA was significantly reduced only by the syn-tasiRNA construct (Figure S3B).

For exogenous application of dsRNAs, 402-, 472- and 420-bp fragments of *GUS*, TSWV-L and TSWV-M were cloned in sense and antisense orientations in a T7 promoter-containing vector for in vitro transcription (Figure S4A). Approximately 10 µg of dsRNAs, generated by annealing in vitro-transcribed single-stranded RNAs (ssRNAs), were gently rubbed onto one leaf of six tomato plants before TSWV inoculation. As before, symptom development was monitored over 28 days. At 12 dpi, half of the plants co-inoculated with TSWV-M dsRNAs remained

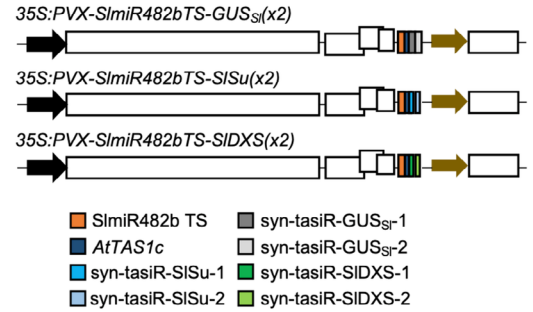
asymptomatic, whereas control plants treated with *GUS* dsRNAs and those co-inoculated with TSWV-L dsRNAs displayed typical TSWV symptoms (Figure S4B,C). At this same time

point, western blot analysis showed no detectable TSWV accumulation in three plants treated with TSWV-M dsRNAs, while high viral levels were observed in controls and in plants

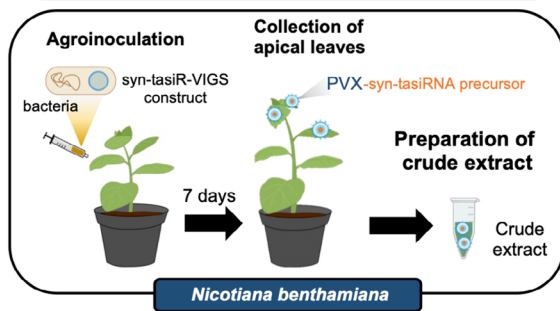
### A Configuration of SlmiR482b-based minimal syn-tasiRNA cassettes



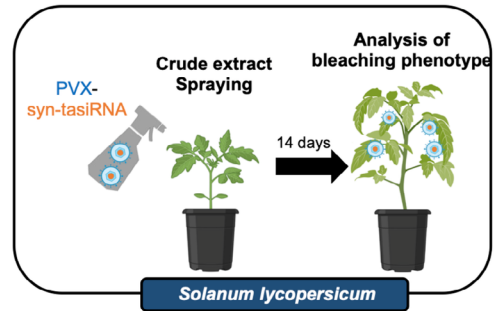
### B PVX-based syn-tasiRNA constructs



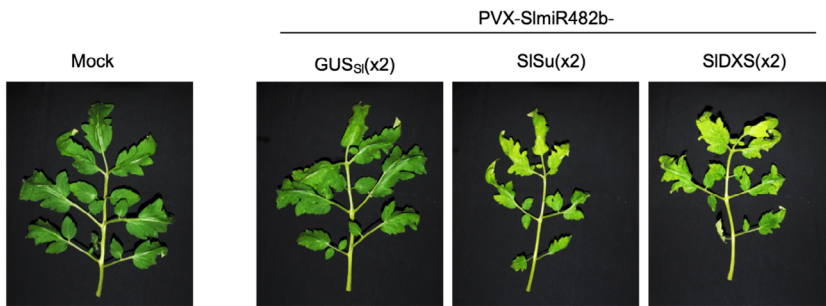
### C Generation of syn-tasiR-VIGS crude extract



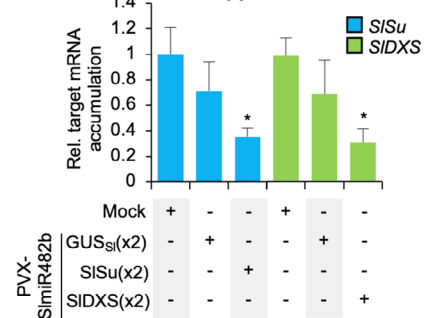
### Transgene-free syn-tasiR-VIGS



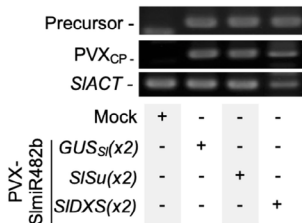
### D Silencing phenotypes in tomato plants inoculated with syn-tasiR-VIGS crude extracts



### E Target mRNA accumulation in upper leaves



### F RT-PCR analysis



### G syn-tasiRNA accumulation in upper leaves



FIGURE 6 | Legend on next page.

**FIGURE 6** | Transgene-free gene silencing through PVX-based syn-tasiR-VIGS in *Solanum lycopersicum*. (A) Schematic representation of PVX-based constructs. Nucleotides of anti-*SlSu* syn-tasiRNAs (syn-tasiR-*SlSu*-1 and syn-tasiR-*SlSu*-2) are shown in dark and light blue, respectively. Nucleotides of anti-*SIDXS* syn-tasiRNAs (syn-tasiR-*SIDXS*-1 and syn-tasiR-*SIDXS*-2) are shown in dark and light green, respectively. Other details are as in Figures 1A and 5A. (B) Diagram of PVX-based constructs expressing anti-*SlSu*, anti-*SIDXS* or anti-*GUS* syn-tasiRNAs. Colour coding for the syn-tasiRNA sequences is consistent with panel (A). Other details are as in Figures 1A and 5A. (C) Experimental procedure for transgene-free syn-tasiR-VIGS in *S. lycopersicum*. Left: Crude extracts are prepared from *Nicotiana benthamiana* plants previously agroinfiltrated with the corresponding syn-tasiR-VIGS construct. Right: Young tomato plants are spray-inoculated with syn-tasiR-VIGS crude extracts to induce bleaching associated with *SlSu* or *SIDXS* silencing. (D) Representative photographs of tomato leaves at 14 days post-spray (dps), from plants sprayed with different crude extracts obtained from agroinoculated *N. benthamiana* plants. (E) Accumulation of *SlSu* and *SIDXS* mRNA in tomato plants treated with syn-tasiR-VIGS crude extracts. Data are presented as the mean + SE relative expression levels of *SlSu* or *SIDXS* mRNA at 14 dps after normalisation to *Actin* (*SLACT*), as determined by RT-qPCR (Mock = 1 in all comparisons). The asterisk indicates a significant difference from the mock samples ( $p < 0.05$ ; pairwise Student's *t*-test comparison). (F) RT-PCR detection at 14 dps of *SlmiR482bTS*-based precursors and PVX coat protein fragment (PVX-CP) in apical leaves of sprayed plants. RT-PCR amplification of *SLACT* is included as a control. (G) Northern blot detection of anti-*SlSu* and anti-*SIDXS* syn-tasiRNAs in RNA preparations from apical leaves collected at 14 dps. A cocktail of probes to simultaneously detect syn-tasiR-*SlSu*-1, syn-tasiR-*SlSu*-2, syn-tasiR-*SIDXS*-1 and syn-tasiR-*SIDXS*-2 was used. Other details are as described in Figure 1C.

treated with TSWV-L dsRNAs (Figure S4D). By 28 dpi, three plants treated with TSWV-M dsRNAs remained symptom-free (Figure S4B). Overall, these experiments demonstrate that exogenous dsRNAs targeting the TSWV M segment can protect tomato plants from infection with an efficiency comparable to that achieved with syn-tasiR-VIGS, whereas dsRNAs directed against the TSWV L segment provide no protection. Taken together, our comparative analyses indicate that syn-tasiR-VIGS is at least as effective as other established RNAi strategies, including MIGS and the exogenous application of dsRNAs.

### 3 | Discussion

In this study, we show that minimal syn-tasiRNA precursors, consisting of only a 22-nt *SlmiR482b* TS and an 11-nt spacer, generate high levels of accurately processed syn-tasiRNAs in *Solanum lycopersicum*, allowing efficient gene silencing in both stable and transient, transgene-free applications. Our findings establish a robust and optimised syn-tasiRNA platform in tomato, overcoming limitations associated with classic RNAi technologies and expanding the potential applications of syn-tasiRNAs in functional genomics and crop improvement.

The successful adaptation of syn-tasiRNA technology to tomato using minimal precursors targeted by endogenous 22-nt miRNAs significantly advances RNAi-based gene silencing tools for crops. Previous studies have reported the efficacy of transgenically expressed syn-tasiRNAs derived from full-length *TAS* precursors in silencing endogenous genes in model species such as *Arabidopsis thaliana* and *N. benthamiana* (Felippes and Weigel 2009; de la Luz Gutierrez-Nava et al. 2008; Montgomery, Howell, et al. 2008; Montgomery, Yoo, et al. 2008). More recently, *TAS*-based syn-tasiRNAs were used to confer antiviral resistance in tomato (Carbonell, Lisón, and Daròs 2019). However, *AtTAS1c*-based syn-tasiRNA constructs require co-expression of *AtMIR173a* in non-*Arabidopsis* species, adding complexity to their implementation in crops such as tomato and *N. benthamiana*. Recent research has shown that minimal syn-tasiRNA precursors targeted by 22-nt miRNAs can generate authentic syn-tasiRNAs in *N. benthamiana* (Cisneros et al. 2025). Here,

we extended this strategy to tomato, using the endogenous 22-nt miRNAs *SlmiR482b* and *SlmiR6020*, both of which trigger secondary siRNA production from target transcripts (Deng, Wang, et al. 2018; Shivaprasad et al. 2012). Our results show that precursors targeted by *SlmiR482b* produced higher syn-tasiRNA levels than those targeted by *SlmiR6020*, most likely because of the stronger expression of *SlmiR482b* in these samples (Figure S5). This is consistent with previous observations in *N. benthamiana*, where *NbmiR482a* was expressed to higher levels than *NbmiR6019a/b*, inducing high syn-tasiRNA production (Cisneros et al. 2025). Furthermore, syn-tasiRNA accumulation from full-length *AtTAS1c* precursors was comparable in leaves overexpressing *AtmiR173a* and in those using *SlmiR482b* as the trigger (Figure 1B), suggesting that *SlmiR482b* levels are not a limiting factor in tomato. Since miRNA expression varies across tissues, developmental stages, and environmental conditions (Jones-Rhoades et al. 2006), selecting an optimal endogenous miRNA trigger is crucial for precise syn-tasiRNA biogenesis. Future studies could explore tissue- or stress-specific expression of endogenous miRNAs to enhance spatiotemporal control of syn-tasiRNA production in crops. Finally, the consistent delay in flowering, accompanied by strong *SFT* transcript reduction in several independent transgenic tomato lines expressing syn-tasiR-*SISFT* from a *SlmiR482b*-based minimal precursor, indicates that the transgenic approach is highly efficient, particularly given that flowering time phenotypes in tomato are much more subtle than in other plant species.

A key feature of syn-tasiRNA technology is its high specificity, as 21-nt guide sequences are computationally designed based on target specificity, minimising off-target effects (Fahlgren et al. 2016; Ossowski et al. 2008). In contrast, larger *TAS*-based systems generate heterogeneous populations of secondary siRNAs from gene fragments inserted after the 22-nt miRNA TS (Felippes and Weigel 2009; Zhao et al. 2024), which can lead to unintended molecular interactions and off-target phenotypes. Here, our high-throughput sequencing data confirm that minimal precursors are accurately processed in tomato, yielding authentic and correctly phased syn-tasiRNAs that accumulate at high levels relative to other sRNAs derived from the precursor (Figure 4B). Furthermore, 21-nt syn-tasiRNAs accumulate in plants treated with syn-tasiR-VIGS constructs

or crude extracts, indicating efficient production from PVX-SlmiR482bTS-based vectors, in line with previous findings in *N. benthamiana* using PVX-NbmiR482aTS-based vectors (Cisneros et al. 2025). Importantly, the absence of resistance in plants expressing 35S:PVX-*AtmiR173aTS-TSWV(x4)* further supports that viral protection resulted from syn-tasiRNA activity rather than from potential siRNAs generated from the minimal precursor during PVX replication. In any case, the efficacy of syn-tasiR-VIGS in tomato allows both complete antiviral resistance (Figure 5) and strong silencing of endogenous genes such as *SISu* and *SIDXs*, resulting in the characteristic leaf-bleaching phenotype (Figure 6). Additional attempts to generate agronomically relevant traits –such as compact growth, early flowering, or increased branching–targeted *SELF-PRUNING (SlSP)*, *SlSP5G*, and *CAROTENOID CLEAVAGE DIOXYGENASE 8 (SlCCD8)* with 2–4 syn-tasiRNAs (Figure S6A) delivered with PVX (Figure S6B) produced the expected phenotypes (Figure S6C,D) with target mRNA levels being reduced (Figure S6D). However, these phenotypes were more subtle than those observed in mutants or stable transgenic lines (Cao et al. 2016; Kohlen et al. 2012), suggesting that obtaining certain traits may require near-complete loss of gene function.

The relative efficiency of syn-tasiRNA technology compared to other RNAi strategies has not been reported, apart from a single study showing that anti-TSWV syn-tasiRNAs conferred stronger protection than an anti-TSWV amiRNA in transgenic tomato, owing to the combined action of multiple syn-tasiRNAs that minimises the likelihood of simultaneous viral escape mutations (Carbonell, Lisón, and Daròs 2019). Here, we tested exogenous dsRNAs containing TSWV L- or M-segment sequences and found that while half of the plants treated with TSWV-M dsRNAs were resistant, all plants treated with TSWV-L dsRNAs remained susceptible (Figure S4). These results agree with a previous report indicating that the efficacy of dsRNA-based resistance against TSWV depends strongly on target region selection (Tabein et al. 2020), and suggest that, when effective, dsRNAs can induce resistance levels comparable to syn-tasiR-VIGS. On the other hand, we also compared the ability of MIGS and syn-tasiRNA constructs to silence endogenous tomato genes in transient expression assays. Both approaches efficiently down-regulated *SISu*, but only the syn-tasiRNA construct significantly reduced *SIDXs* transcript levels (Figure S3B). Together, these results suggest that syn-tasiRNA technology matches or can surpass the performance of other well-established RNAi strategies such as MIGS, reported here for the first time in *S. lycopersicum*, although broader comparative analyses are required to fully define their relative efficacies.

The use of minimal syn-tasiRNA precursors offers several biotechnological advantages. First, shorter syn-tasiRNA precursors reduce construct synthesis costs, making them ideal for large-scale applications that require multiple art-sRNA constructs (Hauser et al. 2013; Jover-Gil et al. 2014; Zhang et al. 2018). Here, SlmiR482b-targeted precursors were integrated into a new series of B/c vectors optimised for cost-effective, high-throughput cloning of syn-tasiRNAs for tomato. This Gateway-compatible and direct binary vector cloning system allows rapid syn-tasiRNA deployment while simplifying construct generation, addressing one of the primary challenges in previous

RNA-based technologies. In particular, our optimised B/c system allows for easy customisation and integration of different promoter and terminator elements in the *pENTR-SlmiR482bTS--B/c* vector. Second, minimal syn-tasiRNA precursors can improve the efficiency of in vitro or bacterial synthesis, facilitating their large-scale production for use in topical application to plants. Third, minimal syn-tasiRNA precursors included in PVX remain stable in treated tomato plants, whereas full-length *TAS*-based precursors are often lost during extended infections (Cisneros et al. 2025). The compact size of minimal precursors may be particularly convenient when using viral vectors with limited cargo capacity. And fourth, syn-tasiR-VIGS allows for the application of syn-tasiRNAs through crude extract spraying, providing a non-transgenic, scalable method for delivering highly specific art-sRNA molecules to plants. It is important to note that the efficacy of our syn-tasiR-VIGS approach, particularly for inducing anti-TSWV resistance, depends on selecting validated syn-tasiRNAs with proven specificity (Carbonell, Lopez, and Daròs 2019). This compensates for producing fewer but highly efficient syn-tasiRNAs, unlike larger *TAS* systems that generate uncontrolled secondary siRNAs from gene fragments, as explained before.

Despite its biotechnological potential, several aspects of syn-tasiRNA technology require further study. Currently, syn-tasiRNA minimal precursors are species-specific; therefore, identifying an efficient endogenous 22-nt miRNA trigger for each plant species remains essential. Regarding syn-tasiR-VIGS, alternative viral vectors beyond PVX should be explored to extend syn-tasiR-VIGS to non-*Solanaceae* crops. As with all VIGS approaches, potential challenges include off-target effects due to viral vector infection, inconsistent efficiency depending on the plant species, tissues, and environmental conditions, and vector mutations during prolonged infections that could compromise efficacy (Rössner et al. 2022). Finally, the integration of syn-tasiRNA technology into commercial breeding programmes will require navigating regulatory frameworks for RNA-based technologies. While RNAi is generally considered a non-GMO approach, regulations vary internationally, particularly regarding the use of recombinant viral vectors for delivery. Addressing these regulatory challenges and developing clear guidelines will be critical for the commercialisation of syn-tasiRNA-based products.

In conclusion, our study establishes a functional and versatile syn-tasiRNA system in tomato, providing a new platform for precision RNAi in both stable and transgene-free applications. Future research should focus on expanding syn-tasiRNA applications across multiple crops, optimising delivery strategies, and addressing regulatory considerations to facilitate the widespread adoption of this promising RNA-based technology in agriculture.

## 4 | Materials and Methods

### 4.1 | Plant Species and Growing Conditions

*S. lycopersicum* cv MoneyMaker and *N. benthamiana* plants were grown in a controlled growth chamber at 25°C, with a 12h light/12h dark photoperiod. Plants were photographed

using a Nikon D3000 digital camera equipped with an AF-S DX NIKKOR 18–55 mm f/3.5–5.6G VR lens.

## 4.2 | Generation of Tomato cv. Moneymaker Transgenic Plants

*Agrobacterium tumefaciens* LBA4404 transformed with 35S:syn-tasiR-SLSFT was co-cultured with tomato cotyledons. Explant preparation, selection, and regeneration were performed as previously described (Ellul et al. 2003). Transformants were selected in hygromycin-containing medium, then transferred to soil for propagation, seed production, and phenotypic and molecular analyses. Non-transgenic controls (NTCs) were in vitro-regenerated tomato plants obtained in parallel with the transgenic plants. Phenotyping was conducted using five NTCs and six independent syn-tasiRNA lines. Flowering time was assessed by counting the number of leaves at the emergence of the first inflorescence.

## 4.3 | Plant Phenotyping

Transgenic plants were phenotyped using five NTCs and six independent syn-tasiRNA lines. Flowering time was assessed by counting the number of leaves at the emergence of the first inflorescence. For syn-tasiR-VIGS experiments, phenotyping included six independently agroinoculated plants. The branching phenotype was determined by counting axillary branches below the first inflorescence; nodes were counted between the second and third inflorescences, and days to flowering were recorded as the number of days from agroinoculation to the first open flower.

## 4.4 | Artificial Small RNA Design

P-SAMS script (<https://github.com/carringtonlab/psams>) (Fahlgren et al. 2016), configured to return unlimited optimal results, was used to obtain a list of optimal amiRNAs targeting *SlSu*, *SIDXS*, *SISP*, *SISP5G* and *SICCD8* with high specificity (Data S2). Off-target filtering was applied using the *S. lycopersicum* transcriptome iTAGv4.0 ([https://solgenomics.net/ftp/tomato\\_genome/annotation/ITAG4.0\\_release/](https://solgenomics.net/ftp/tomato_genome/annotation/ITAG4.0_release/)) (Hosmani et al. 2019) to enhance syn-tasiRNA specificity. The guide sequences for syn-tasiR-NbSu, syn-tasiR-GUS<sub>Nb</sub>, syn-tasiR-SLSFT, syn-tasiR-GUS<sub>S1</sub>-1, syn-tasiR-GUS<sub>S1</sub>-2, syn-tasiR-TSWV-1, syn-tasiR-TSWV-2, syn-tasiR-TSWV-3 and syn-tasiR-TSWV-4 were described before (Carbonell, Lopez, and Daròs 2019; Carbonell and Daròs 2017; Cisneros et al. 2022; Shalit et al. 2009).

## 4.5 | DNA Constructs

Oligonucleotides AC-902/AC-903 including *SlmiR482b* targeted precursor were annealed and ligated into *BsaI*-digested *pENTR-B/c* and *pMDC32B-B/c* to generate *pENTR-SlmiR482bTS-BB* and *pMDC32B-SlmiR482bTS-BB*, respectively. The B/c cassette was excised from *BsaI*-digested *pMDC32B-AtTAS1c-D2-B/c*

(Addgene plasmid #137884) (López-Dolz et al. 2020) and ligated into *BsaI*-digested *pENTR-SlmiR482bTS-BB* and *pMDC32B-SlmiR482bTS-BB* to generate *pENTR-SlmiR482bTS-B/c* and *pMDC32B-SlmiR482bTS-B/c*. These new B/c vectors *pENTR-SlmiR482bTS-B/c* (Addgene plasmid #234368) and *pMDC32B-SlmiR482bTS-B/c* (Addgene plasmid #234369) were deposited in Addgene.

Constructs 35S:*SlmiR482b-GUS<sub>S1</sub>*, 35S:*SlmiR482b-NbSu*, 35S:*SlmiR6019-GUS<sub>S1</sub>*, 35S:*SlmiR6019-NbSu*, 35S:*SlmiR482b-SlSu(x2)*, 35S:*SlmiR482b-SIDXS(x2)*, 35S:*SlmiR482b-GUS<sub>S1</sub>(x2)*, and 35S:*SlmiR482b-SLSFT* were obtained by ligating annealed oligonucleotide pairs AC-824/AC-825-AC-826/AC-827-AC-828/AC-829-AC-830/AC-831-AC-892/AC-893-AC-894/AC-895-AC-915/AC-916 and AC-909/AC-910 into *pMDC32B-B/c* (Addgene plasmid #227963) (Cisneros et al. 2025) and *pMDC32B-SlmiR482bTS-B/c*, respectively, as described (Carbonell et al. 2014) (Figure S1). A detailed protocol for cloning syn-tasiRNAs in B/c vectors including *SlmiR482b TS* is described in Text S1.

For PVX-based constructs, syn-tasiRNA cassettes *AtmiR173aTS-TSWV(x4)*, *SlmiR482bTS-GUS<sub>S1</sub>(x2)*, *SlmiR482bTS-SlSu(x2)*, *SlmiR482bTS-SIDXS(x2)*, *SlmiR482bTS-SISP(x4)*, *SlmiR482bTS-SISP5G(x2)-SISP(x2)*, and *SlmiR482bTS-SICCD8(x4)* were synthesised as dsDNA oligonucleotides AC-1205, AC-993, AC-775, AC-776, AC-1325, AC-1327 and AC-1328, respectively, and assembled into *MluI*-digested and gel-purified *pLBPVXBa-M* (Addgene plasmid #229079) (30) in the presence of GeneArt Gibson Assembly HiFi Master Mix (Invitrogen) to generate 35S:*PVX-AtmiR173aTS-TSWV(x4)*, 35S:*PVX-SlmiR482bTS-GUS<sub>S1</sub>(x2)*, 35S:*PVX-SlmiR482bTS-SlSu(x2)*, 35S:*PVX-SlmiR482bTS-SIDXS(x2)*, 35S:*PVX-SlmiR482bTS-SISP(x4)*, 35S:*PVX-SlmiR482bTS-SISP5G(x2)-SISP(x2)* and 35S:*PVX-SlmiR482bTS-SICCD8(x4)*, respectively. Text S2 provides a detailed protocol for cloning syn-tasiRNA *SlmiR482bTS*-based minimal precursors into *pLBPVXBa-M*.

For MIGS constructs, gene fragments of *GUS* (402 bp), *SlSu* (414 bp) and *SIDXS* (413 bp), each preceded by the *SlmiR482b* target site sequence (*SlmiR482bTS*), were PCR-amplified with oligonucleotides AC-1329/AC-1330, AC-1331/AC-1332 and AC-1333/AC-1334, respectively, using *pMDC99-GUS* (Carbonell et al. 2012) or tomato cDNA as template. The resulting products were cloned into *pENTR-D-TOPO* (Thermo Fisher Scientific) and transferred by LR recombination into *pMDC32* (Curtis and Grossniklaus 2003) to generate 35S:*SlmiR482bTS-GUS(MIGS)*, 35S:*SlmiR482bTS-SlSu(MIGS)* and 35S:*SlmiR482bTS-SIDXS(MIGS)* constructs.

For dsRNA-generating constructs, gene fragments of *GUS* (402 bp), *TSWV-L* (472 bp) and *TSWV-M* (420 bp) were PCR-amplified with oligonucleotides AC-1330/AC-1335, AC-1170/AC-1171 and AC-1338/AC-1339, respectively, using *pMDC99-GUS* (Carbonell et al. 2012) or *TSWV*-infected tomato cDNA as the template. The PCR products were cloned in both orientations into a *pUC18* (Yanisch-Perron et al. 1985) derivative including a T7 promoter followed by an *EcoRV* site (Carbonell et al. 2008) to generate *T7:GUS(+)*, *T7:GUS(-)*, *T7:TSWV-L(+)*, *T7:TSWV-L(-)*, *T7:TSWV-M(+)* and *T7:TSWV-M(-)* constructs.

35S:*AtTAS1c-NbSu/MIR173*, 35S:*PVX-NbmiR482aTS-GUSsl(x4)* and 35S:*PVX-NbmiR482aTS-TSWV(x4)* were described before (Cisneros et al. 2025; López-Dolz et al. 2020). All DNA oligonucleotides used in this study are listed in Table S1. The sequences of all syn-tasiRNA precursors are listed in Text S3. The sequences of newly developed B/c vectors are listed in Text S4.

#### 4.6 | Transient Expression of Constructs and Inoculation of Viruses

*Agrobacterium*-mediated infiltration of DNA constructs in *N. benthamiana* and *S. lycopersicum* leaves was done as previously (Carbonell et al. 2015; Cuperus et al. 2010). Preparation of crude extracts obtained from virus-infected *N. benthamiana* plants was done as previously (Cisneros, Martín-García, et al. 2023; Cisneros et al. 2025). Syn-tasiR-VIGS extracts were sprayed onto *S. lycopersicum* leaves, and TSWV was mechanically inoculated by gently rubbing the leaf surface (Carbonell, Lopez, and Daròs 2019; Cisneros et al. 2025).

#### 4.7 | Total RNA Preparation

Total RNA from *S. lycopersicum* leaves was isolated as previously described (Cisneros, Lisón, et al. 2023). Triplicate samples from pools of two leaves were analysed.

#### 4.8 | In Vitro Transcription and dsRNA Generation

dsRNAs were prepared by annealing complementary ssRNAs generated by in vitro transcription of *pUC18*-based recombinant plasmids with the TranscriptAid T7 kit (Thermo Fisher Scientific) according to the manufacturer's instructions. Briefly, 2 µg of each plasmid was linearised by *Xba*I restriction digestion. 1 µg of purified digested plasmid was used in a 20 µL transcription reaction containing 4 µL of 5X TranscriptAid Reaction Buffer, 8 µL of 25 mM NTP mix and 2 µL of TranscriptAid Enzyme Mix, which was incubated at 37°C for 2 h. After removing the DNA template by DNase I digestion and purification of ssRNAs by a phenol:chloroform:isoamyl alcohol extraction, equal amounts of sense and antisense ssRNAs were mixed, heated to 95°C for 3 min, and allowed to cool slowly to 30°C. Successful annealing was verified by the characteristic shift in electrophoretic mobility on non-denaturing agarose gels.

#### 4.9 | Real-Time RT-qPCR

Real time RT-qPCR was performed using the same RNA samples as those used for sRNA-blot analysis, as described (Cisneros et al. 2025). Oligonucleotides used for RT-qPCR are listed in Table S1. Target mRNA expression levels were calculated relative to the reference gene *SLACT* using the delta cycle threshold comparative method in QuantStudio Design and Analysis software (version 1.5.1, Thermo Fisher Scientific). Three independent biological replicates were analysed, each with two technical replicates.

#### 4.10 | Stability of Syn-tasiRNA Precursors During Viral Infections

Total RNA from apical leaves of the three biological replicates was pooled prior to cDNA synthesis. PCR detection of syn-tasiRNA precursors, PVX, and *SLACT* was performed using oligonucleotide pairs AC-654/AC-655, AC-657/AC-658, and AC-280/AC-281 (Table S1), respectively, with Phusion DNA polymerase (ThermoFisher Scientific). PCR products were analysed by agarose gel electrophoresis.

#### 4.11 | Small RNA Blot Assays

Total RNA (20 µg) was separated in 17% polyacrylamide gels containing 0.59 Tris/Borate EDTA and 7 M urea and transferred to a positively charged nylon membrane. Synthesis of DNA or LNA oligonucleotide probes labelled with the second-generation DIG Oligonucleotide 3'-End Labelling Kit (Roche) and membrane hybridisation at 38°C were done as described (Tomassi et al. 2017). An ImageQuant 800 CCD imager (Cytiva) was used to produce digital images from membranes, and band quantification was done using ImageQuant TL version 10.2 (Cytiva). Oligonucleotides used as probes for sRNA blots are listed in Table S1.

#### 4.12 | Small RNA Sequencing and Data Analysis

Total RNA quantity, purity, and integrity were assessed using a 2100 Bioanalyzer (RNA 6000 Nano kit, Agilent) before submission to BGI (Hong Kong, China) for sRNA library preparation and SE50 high-throughput sequencing on a DNBSEQ-G-400 sequencer. Quality-trimmed reads with adaptor removed, as received from BGI, were processed using the fastx\_collapser toolkit (<http://hannonlab.cshl.edu/fastxtoolkit>) (Hannon 2010) to merge identical sequences while retaining read counts. Each unique, cleaned read was mapped to the forward strand of the corresponding syn-tasiRNA precursor expressed in each sample (Data S3) using a custom Python script, ensuring exact matches with no gaps or mismatches. The script also calculated read counts and RPMs (reads per million mapped reads) for each mapped position.

To evaluate the processing accuracy of syn-tasiRNA precursors, we quantified the proportion of 19–24 nt sRNA (+) reads mapping within ±4 nt of the 5' end of the syn-tasiRNA guide, as previously described (Carbonell et al. 2015; Cuperus et al. 2010). Additionally, phasing register tables were generated by determining the percentage of 21-nt sRNA (+) reads in each register relative to the predicted syn-tasiRNA cleavage site, considering all 21-nt positions downstream of the cleavage site, following established methods (Carbonell et al. 2014; Cisneros et al. 2025).

#### 4.13 | 5'-RLM-Race

RNA ligase-mediated rapid amplification of 5' cDNA ends (5'-RLM RACE) was performed using the GeneRacer kit (Life Technologies), essentially as described (Carbonell et al. 2015).

Specifically, first-round PCR amplification was done with the GeneRacer 5' and gene-specific AC-1251 oligonucleotides, followed by a second round PCR using the GeneRacer 5' nested and AC-1252 oligonucleotides. The resulting 5'-RLM-RACE products were gel-purified, cloned using the Zero Blunt TOPO PCR Cloning Kit (Life Technologies), transformed into *Escherichia coli* DH5 $\alpha$ , and screened for inserts before sequencing. Control PCR reactions to amplify *SISFT* and *SLACT* were done using oligonucleotide pairs AC-1250/AC-1252 and AC-280/AC-281, respectively. A complete list of the oligonucleotides used is provided in Table S1.

#### 4.14 | Protein Blot Analysis

Protein separation, membrane transfer, antibody incubation, and target protein detection were performed as previously described (Cisneros et al. 2025). To assess overall protein content, membranes were stained with Ponceau red S solution (Thermo Fisher Scientific).

#### 4.15 | Statistical Analysis

The statistical analyses used are detailed in the figure legends. Significant differences were assessed using a two-tailed Student's *t*-test.

#### 4.16 | Gene and Virus Identifiers

The gene identifiers for *N. benthamiana* and *S. lycopersicum* are as follows: *NbSu* (Nbv5.1tr6204879), *SLACT* (Solyc04g011500.3.1), *SIDXS1* (Solyc01g067890), *SISFT* (Solyc03g063100.2.1), *SISu* (Solyc10g008740), and *SITIP41* (SGN-U584254). The genome identifiers for the TSWV LL-N.05 segment L, M, and S are KP008128, FM163373, and KP008129, respectively. PVX-based constructs include PVX sequence variant MT799816.1. *Escherichia coli*  $\beta$ -glucuronidase gene sequence corresponds to GenBank accession number S69414.1.

#### Author Contributions

A.H.T., and M.J.-M. did most of the experimental work with the help of A.E.C., A.A., F.O. and S.T.-F., S.P., A.G. and A.A. generated and maintained the transgenic tomato lines. A.H.T., M.J.-M., A.E.C. and A.C. analysed the data. A.C. conceived the research, supervised the project, and wrote the manuscript with input from the rest of the authors.

#### Acknowledgements

We thank Javier Forment (IBMCP) for his support with sRNA sequencing data analysis, Alejandro Atarés (IBMCP) for sharing greenhouse space, and the IBMCP greenhouse staff for their assistance in plant maintenance. This work was supported by grants or fellowships from MCIN/AEI/10.13039/501100011033 and/or by the "European Union NextGenerationEU/PRTR" [PID2024-155602OB-I00, PID2021-122186OB-I00, PDC2022-133241-I00 and CNS2022135107 to A.C.; PRE2019-088439 and PRE2022103177 to A.E.C. and M.J.-M., respectively], and from the European Union's Horizon Europe research and innovation programme under the Marie Skłodowska-Curie grant agreement No 101149036 (HORIZON-MSCA-2023-PF-01-101149036 to A.H.T.).

#### Conflicts of Interest

The authors declare no conflicts of interest.

#### Data Availability Statement

All original data will be made available upon request. High-throughput sequencing data can be found in the Sequence Read Archive (SRA) database under accession number PRJNA1220650. New B/c and vectors are available from Addgene: *pENTR-SlmiR482bTS-B/c* (Addgene plasmid #234368, <https://www.addgene.org/234368>), *pMDC32B-SlmiR482bTS-B/c* (Addgene plasmid #234369, <https://www.addgene.org/234369>).

#### References

- Allen, E., Z. Xie, A. M. Gustafson, and J. C. Carrington. 2005. "microRNA-Directed Phasing During Trans-Acting siRNA Biogenesis in Plants." *Cell* 121: 207–221.
- Bartel, D. P. 2004. "MicroRNAs: Genomics, Biogenesis, Mechanism, and Function." *Cell* 116: 281–297.
- Baulcombe, D. 2004. "RNA Silencing in Plants." *Nature* 431: 356–363.
- Bernard, P., and M. Couturier. 1992. "Cell Killing by the F Plasmid CcdB Protein Involves Poisoning of DNA-Topoisomerase II Complexes." *Journal of Molecular Biology* 226: 735–745.
- Bernstein, E., A. A. Caudy, S. M. Hammond, and G. J. Hannon. 2001. "Role for a Bidentate Ribonuclease in the Initiation Step of RNA Interference." *Nature* 409: 363–366.
- Cao, K., L. Cui, X. Zhou, L. Ye, Z. Zou, and S. Deng. 2016. "Four Tomato FLOWERING LOCUS T-Like Proteins Act Antagonistically to Regulate Floral Initiation." *Frontiers in Plant Science* 6: 1213.
- Carbonell, A. 2017. "Artificial Small RNA-Based Strategies for Effective and Specific Gene Silencing in Plants." In *Plant Gene Silencing: Mechanisms and Applications*, edited by T. Dalmay, 110–127. CABI Publishing.
- Carbonell, A., and J.-A. Daròs. 2017. "Artificial microRNAs and Synthetic Trans-Acting Small Interfering RNAs Interfere With Viroid Infection." *Molecular Plant Pathology* 18: 746–753.
- Carbonell, A., N. Fahlgren, H. Garcia-Ruiz, et al. 2012. "Functional Analysis of Three Arabidopsis ARGONAUTES Using Slicer-Defective Mutants." *Plant Cell* 24: 3613–3629.
- Carbonell, A., N. Fahlgren, S. Mitchell, et al. 2015. "Highly Specific Gene Silencing in a Monocot Species by Artificial microRNAs Derived From Chimeric miRNA Precursors." *Plant Journal* 82: 1061–1075.
- Carbonell, A., P. Lisón, and J.-A. Daròs. 2019. "Multi-Targeting of Viral RNAs With Synthetic Trans-Acting Small Interfering RNAs Enhances Plant Antiviral Resistance." *Plant Journal* 100: 720–737.
- Carbonell, A., C. Lopez, and J.-A. Daròs. 2019. "Fast-Forward Identification of Highly Effective Artificial Small RNAs Against Different Tomato Spotted Wilt Virus Isolates." *Molecular Plant-Microbe Interactions* 32: 142–156.
- Carbonell, A., A. E. Martinez de Alba, R. Flores, and S. Gago. 2008. "Double-Stranded RNA Interferes in a Sequence-Specific Manner With the Infection of Representative Members of the Two Viroid Families." *Virology* 371: 44–53.
- Carbonell, A., A. Takeda, N. Fahlgren, S. C. Johnson, J. T. Cuperus, and J. C. Carrington. 2014. "New Generation of Artificial MicroRNA and Synthetic Trans-Acting Small Interfering RNA Vectors for Efficient Gene Silencing in Arabidopsis." *Plant Physiology* 165: 15–29.
- Chen, H.-M., L.-T. Chen, K. Patel, Y.-H. Li, D. C. Baulcombe, and S.-H. Wu. 2010. "22-Nucleotide RNAs Trigger Secondary siRNA Biogenesis in Plants." *PNAS* 107: 15269–15274.
- Cisneros, A. E., A. Alarcia, J. J. Llorens-Gámez, et al. 2025. "Syn-tasiR-VIGS: Virus-Based Targeted RNAi in Plants by Synthetic Trans Acting

- Small Interfering RNAs Derived From Minimal Precursors." *Nucleic Acids Research* 53: gkaf183.
- Cisneros, A. E., A. de la Torre-Montaña, and A. Carbonell. 2022. "Systemic Silencing of an Endogenous Plant Gene by Two Classes of Mobile 21-Nucleotide Artificial Small RNAs." *Plant Journal* 110: 1166–1181.
- Cisneros, A. E., P. Lisón, L. Campos, et al. 2023. "Down-Regulation of Tomato STEROL GLYCOSYLTRANSFERASE 1 Perturbs Plant Development and Facilitates Viroid Infection." *Journal of Experimental Botany* 74: 1564–1578.
- Cisneros, A. E., T. Martín-García, A. Primc, et al. 2023. "Transgene-Free, Virus-Based Gene Silencing in Plants by Artificial microRNAs Derived From Minimal Precursors." *Nucleic Acids Research* 51: 10719–10736.
- Cuperus, J. T., A. Carbonell, N. Fahlgren, et al. 2010. "Unique Functionality of 22-Nt miRNAs in Triggering RDR6-Dependent siRNA Biogenesis From Target Transcripts in Arabidopsis." *Nature Structural & Molecular Biology* 17: 997–1003.
- Curtis, M. D., and U. Grossniklaus. 2003. "A Gateway Cloning Vector Set for High-Throughput Functional Analysis of Genes in Planta." *Plant Physiology* 133: 462–469.
- de la Luz Gutierrez-Nava, M., M. J. Aukerman, H. Sakai, S. V. Tingey, and R. W. Williams. 2008. "Artificial Trans-Acting siRNAs Confer Consistent and Effective Gene Silencing." *Plant Physiology* 147: 543–551.
- Deng, P., S. Muhammad, M. Cao, and L. Wu. 2018. "Biogenesis and Regulatory Hierarchy of Phased Small Interfering RNAs in Plants." *Plant Biotechnology Journal* 16: 965–975.
- Deng, Y., J. Wang, J. Tung, et al. 2018. "A Role for Small RNA in Regulating Innate Immunity During Plant Growth." *PLoS Pathogens* 14: e1006756.
- Ding, S. W., and O. Voinnet. 2007. "Antiviral Immunity Directed by Small RNAs." *Cell* 130: 413–426.
- Ellul, P., B. Garcia-Sogo, B. Pineda, G. Rios, L. A. Roig, and V. Moreno. 2003. "The Ploidy Level of Transgenic Plants in Agrobacterium-Mediated Transformation of Tomato Cotyledons (*Lycopersicon esculentum* Mill.) is Genotype and Procedure Dependent [Corrected]." *Theoretical and Applied Genetics* 106: 231–238.
- Fahlgren, N., S. T. Hill, J. C. Carrington, and A. Carbonell. 2016. "P-SAMS: A Web Site for Plant Artificial microRNA and Synthetic Trans-Acting Small Interfering RNA Design." *Bioinformatics* 32: 157–158.
- Felippes, F. F., and D. Weigel. 2009. "Triggering the Formation of tasiRNAs in *Arabidopsis thaliana*: The Role of microRNA miR173." *EMBO Reports* 10: 264–270.
- Fire, A., S. Xu, M. K. Montgomery, S. A. Kostas, S. E. Driver, and C. C. Mello. 1998. "Potent and Specific Genetic Interference by Double-Stranded RNA in *Caenorhabditis elegans*." *Nature* 391: 806–811.
- Hammond, S. M., E. Bernstein, D. Beach, and G. J. Hannon. 2000. "An RNA-Directed Nuclease Mediates Post-Transcriptional Gene Silencing in *Drosophila* Cells." *Nature* 404: 293–296.
- Hannon, G. J. 2002. "RNA Interference." *Nature* 418: 244–251.
- Hannon, G. J. 2010. "FASTX-Toolkit (RRID:SCR\_005534)." [http://hannonlab.cshl.edu/fastx\\_toolkit](http://hannonlab.cshl.edu/fastx_toolkit).
- Hauser, F., W. Chen, U. Deinlein, et al. 2013. "A Genomic-Scale Artificial microRNA Library as a Tool to Investigate the Functionally Redundant Gene Space in Arabidopsis." *Plant Cell* 25: 2848–2863.
- Hosmani, P. S., M. Flores-Gonzalez, H. van de Geest, et al. 2019. "An Improved de Novo Assembly and Annotation of the Tomato Reference Genome Using Single-Molecule Sequencing, Hi-C Proximity Ligation and Optical Maps." 767764.
- Jackson, A. L., S. R. Bartz, J. Schelter, et al. 2003. "Expression Profiling Reveals Off-Target Gene Regulation by RNAi." *Nature Biotechnology* 21: 635–637.
- Jiang, K., K. L. Liberatore, S. J. Park, J. P. Alvarez, and Z. B. Lippman. 2013. "Tomato Yield Heterosis Is Triggered by a Dosage Sensitivity of the Florigen Pathway That Fine-Tunes Shoot Architecture." *PLoS Genetics* 9: e1004043.
- Jones-Rhoades, M. W., D. P. Bartel, and B. Bartel. 2006. "MicroRNAs and Their Regulatory Roles in Plants." *Annual Review of Plant Biology* 57: 19–53.
- Jover-Gil, S., J. Paz-Ares, J. L. Micol, and M. R. Ponce. 2014. "Multi-Gene Silencing in Arabidopsis: A Collection of Artificial microRNAs Targeting Groups of Paralogs Encoding Transcription Factors." *Plant Journal* 80: 149–160.
- Kohlen, W., T. Charnikhova, M. Lammers, et al. 2012. "The Tomato CAROTENOID CLEAVAGE DIOXYGENASE8 (SICCD8) Regulates Rhizosphere Signaling, Plant Architecture and Affects Reproductive Development Through Strigolactone Biosynthesis." *New Phytologist* 196: 535–547.
- Krieger, U., Z. B. Lippman, and D. Zamir. 2010. "The Flowering Gene SINGLE FLOWER TRUSS Drives Heterosis for Yield in Tomato." *Nature Genetics* 42: 459–463.
- Li, J., Z. Yang, B. Yu, J. Liu, and X. Chen. 2005. "Methylation Protects miRNAs and siRNAs From a 3'-End Uridylation Activity in Arabidopsis." *Current Biology* 15: 1501–1507.
- López-Dolz, L., M. Spada, J.-A. Daròs, and A. Carbonell. 2020. "Fine-Tune Control of Targeted RNAi Efficacy by Plant Artificial Small RNAs." *Nucleic Acids Research* 48: 6234–6250.
- Montgomery, T. A., M. D. Howell, J. T. Cuperus, et al. 2008. "Specificity of ARGONAUTE7-miR390 Interaction and Dual Functionality in TAS3 Trans-Acting siRNA Formation." *Cell* 133: 128–141.
- Montgomery, T. A., S. J. Yoo, N. Fahlgren, et al. 2008. "AGO1-miR173 Complex Initiates Phased siRNA Formation in Plants." *PNAS* 105: 20055–20062.
- Ossowski, S., R. Schwab, and D. Weigel. 2008. "Gene Silencing in Plants Using Artificial microRNAs and Other Small RNAs." *Plant Journal* 53: 674–690.
- Rössner, C., D. Lotz, and A. Becker. 2022. "VIGS Goes Viral: How VIGS Transforms Our Understanding of Plant Science." *Annual Review of Plant Biology* 73: 703–728.
- Shalit, A., A. Rozman, A. Goldshmidt, et al. 2009. "The Flowering Hormone Florigen Functions as a General Systemic Regulator of Growth and Termination." *Proceedings of the National Academy of Sciences* 106: 8392–8397.
- Shivaprasad, P. V., H.-M. Chen, K. Patel, D. M. Bond, B. A. C. M. Santos, and D. C. Baulcombe. 2012. "A MicroRNA Superfamily Regulates Nucleotide Binding Site–Leucine-Rich Repeats and Other mRNAs[W] [OA]." *Plant Cell* 24: 859–874.
- Su, W., M. Xu, Y. Radani, and L. Yang. 2023. "Technological Development and Application of Plant Genetic Transformation." *International Journal of Molecular Sciences* 24: 10646.
- Tabein, S., M. Jansen, E. Noris, et al. 2020. "The Induction of an Effective dsRNA-Mediated Resistance Against Tomato Spotted Wilt Virus by Exogenous Application of Double-Stranded RNA Largely Depends on the Selection of the Viral RNA Target Region." *Frontiers in Plant Science* 11: 533338.
- Tomassi, A. H., D. Gagliardi, D. A. Cambiagno, and P. A. Manavella. 2017. "Nonradioactive Detection of Small RNAs Using Digoxigenin-Labeled Probes." In *Plant Argonaute Proteins: Methods and Protocols*, edited by A. Carbonell, 199–210. Springer.

Yanisch-Perron, C., J. Vieira, and J. Messing. 1985. "Improved M13 Phage Cloning Vectors and Host Strains: Nucleotide Sequences of the M13mpl8 and pUC19 Vectors." *Gene* 33: 103–119.

Yoshikawa, M., A. Peragine, M. Y. Park, and R. S. Poethig. 2005. "A Pathway for the Biogenesis of Trans-Acting siRNAs in Arabidopsis." *Genes & Development* 19: 2164–2175.

Zhang, Y., V. Nasser, O. Pisanty, et al. 2018. "A Transportome-Scale amiRNA-Based Screen Identifies Redundant Roles of Arabidopsis ABCB6 and ABCB20 in Auxin Transport." *Nature Communications* 9: 4204.

Zhang, Z. J. 2014. "Artificial Trans-Acting Small Interfering RNA: A Tool for Plant Biology Study and Crop Improvements." *Planta* 239: 1139–1146.

Zhao, X., Q. Gao, H. Wang, et al. 2024. "Syn-tasiRNAs Targeting the Coat Protein of Potato Virus Y Confer Antiviral Resistance in Nicotiana Benthamiana." *Plant Signaling & Behavior* 19: 2358270.

### Supporting Information

Additional supporting information can be found online in the Supporting Information section. **Data S1:** 21-nt siRNAs from SISFT and SILRR1. **Data S2:** P-SAMS designs of art-sRNA sequences. **Data S3:** sRNA reads from syn-tasiRNA-expressing tissues. **Figure S1:** Direct syn-tasiRNA cloning downstream the SlmiR482b target site (TS) in B/c (BsaI/ccdB)-**Figure S2:** Phasing analysis of 21-nt reads corresponding to SISFT and SISFT. **Figure S3:** Comparative analysis of gene silencing induced by MIGS and syn-tasiRNAs in Solanum. **Figure S4:** Functional analysis of dsRNA treatments against tomato spotted wilt virus (TSWV) in *S. lycopersicum* agroinfiltrated. **Figure S5:** Analysis of SlmiR482b and SlmiR6020 presence in *Solanum lycopersicum* agroinfiltrated. **Figure S6:** Functional analysis PVX-based syn-tasiRNA-VIGS silencing of SlSP/SlSP5G and SlCCD8. **Table S1:** Name, sequence and use of oligonucleotides used in this study. **Text S1:** Protocol to design and clone syn-tasiRNAs downstream the 3'D1[+] position in BsaI/ccdBbased ('B/c') vectors *pENTR-SlmiR482bTS-B/c* and *pMDC32B-SlmiR482bTS-B/c*. **Text S2:** Protocol to generate PVX-based syn-tasiRNA constructs. **Text S3:** DNA sequence in FASTA format of all precursors used to express art-sRNAs in plants. **Text S4:** DNA sequence of BsaI-ccdB-based (B/c) vectors used for direct cloning of syn-tasiRNAs.